Hydrodynamic and Optical Measurements in the Atmospheric Boundary Layer

Scott C. Morris and Stanislav Gordeyev

Final Technical Report

Center for Flow Physics and Control

in the

Hessert Laboratory for Aerospace Research

University of Notre Dame
Notre Dame, IN 46556

Department of Aerospace and Mechanical Engineering

UND-SM07-0327

January 2007

Hydrodynamic and Optical Measurements in the Atmospheric Boundary Layer

Scott C. Morris and Stanislav Gordeyev

Final Technical Report

Contract No. DTRT57-06-P-80144

by the

University of Notre Dame

Notre Dame, Indiana

for the

USDOT Volpe Center

Cambridge, MA

UND-SM07-0327

January 2007

1.0 INTRODUCTION

The Volpe National Transportation Systems Center (Volpe) supports the NASA Wake Vortex program in data collection, analysis and modeling of the airplane wake vortex data to improve operations at a number of airports that experience capacity constraints. As part of the NASA's effort in evaluating emerging wake vortex sensing technologies, a test was carried out at DEN airport during the fall of 2005 to evaluate the state of the Sensor for Optical Characterization of Ring-eddy Atmospherically Emanating Sound (SOCRATES). This sensor uses an array of laser beams acting as a continuous aperture laser microphone to passively detect and track the sound generated by airplane wake vortices.

An apparent limitation of the SOCRATES sensor is its susceptibility to what is referred to as Refractive Index Variability (RIV) noise. This sensor's operation fundamentally relies on the acoustically induced variation of the air refractive index to detect the presence of a sound wave and measure it. However, acoustic waves are not the only phenomenon that affects the air refractive index. Atmospheric temperature and velocity fluctuations along the path of the laser beam also cause a fluctuation in the index of refraction of the air. These fluctuations are so large that they completely mask the acoustic signal in some frequency bands.

Data were taken at Denver International Airport (DEN) during the period of two days, Dec, 15th and Dec, 16th of 2005. Data consists of high frequency velocity data collected using hot-wire anemometers and Sonic anemometers, see Figure 1, as well as simultaneous SOCRATES optical data. The present report documents the data processing and preliminary results of these measurements. Specifically, auto and cross spectral densities of velocity components, temperature fluctuations, and optical aberrations were computed. The results are intended to provide insight into the physical mechanisms responsible for RIV noise, thereby facilitating the development of a statistical model for the effects of RIV on the SOCRATES signals. The long term intent is to use a post-processing methodology that increases the sensitivity of the SOCRATES system to the acousti-

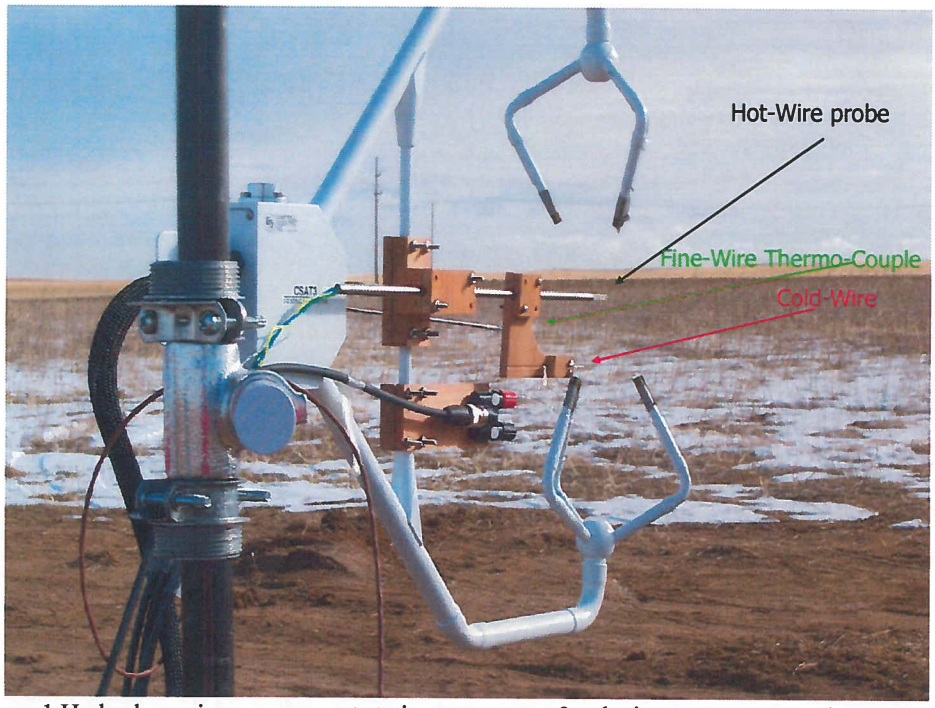

Figure 1 Hydrodynamic measurement station to measure 3 velocity components and temperature

cally generated optical aberrations, and decreases the sensitivity to RIV noise. The following section will describe the calibration, processing and results from these measurements.

2.0 RESULTS

The measurements considered used a three component sonic anemometer, a multi-sensor hot-wire probe, and a cold-wire sensor. The intention was to use the sonic anemometer measurements for in-situ calibration of the hot-wire probe. The data acquired on 15-December were found to be unusable due to highly fluctuating wind directions. This resulted in a condition where the approach velocity vector was not within the normal operating "cone" of the hot-wire probe. The data that were acquired on 16-December were found to be satisfactory for hot-wire calibration. Below only data from Dec, 16th are presented.

2.1 Hydrodynamic Measurement Results

Figure 2 presents a short time (10 sec) averaged temporal evolution of velocity components and temperature for entire measurement period. U-component of velocity is parallel to the hot-wire axis and W and V components are horizontal and vertical cross-stream components, respectively. Temperature fluctuations are the strongest during the first hour of the measurements, then they diminish to almost no fluctuations around 23:00 GMT. At approximately 23:30 GMT a small increase in the high frequency fluctuations was observed, after which the magnitude stayed fairly constant. It will be shown later that these two intervals, before and after 23:00 GMT correspond to two physically different atmospheric conditions. The first interval is before the sunset, when the ground is warmer then the air, which leads to unstable conditions. The second interval is after the sunset, when ground was cooling faster that the air thus creating stable conditions.

Sonic anemometry data were used to calibrate triple hot-wire anemometer in-situ. Sonic data were sampled at the sampling frequency of 60 Hz, while hot-wire anemometry data were sampled at 769 Hz. For calibration, hot wire signals were re-sampled to match sonic data sampling rate.

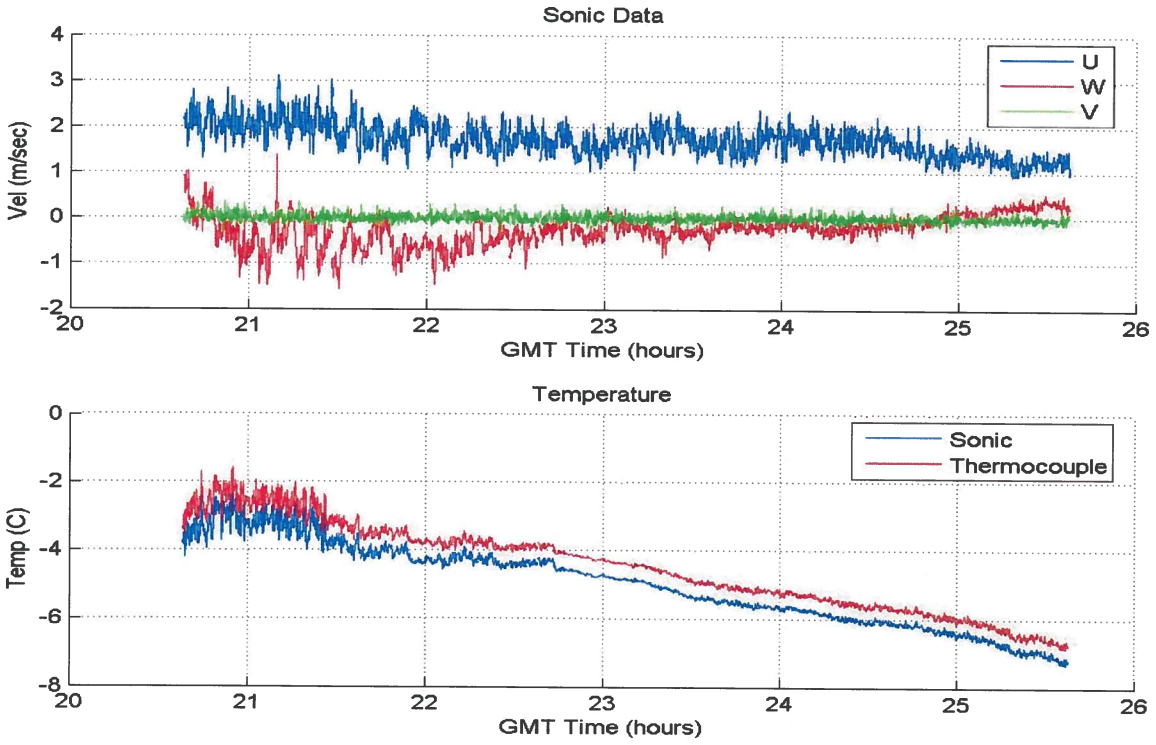

Figure 2 Short time average temporal evolution of wind and temperature.

To calibrate triple hot-wires, an algorithm proposed in [1,2] was used. It assumes the relation between an "effective cooling speed", U_{eff}, and a voltage signal from a hot-wire, E. The effective cooling speed is defined as

$$U_{eff}^2 = U_n^2 + k^2 U_t^2 + h^2 U_b^2 , \quad (1)$$

where U_n, U_t and U_b are the normal, tangential and by-normal velocity components to the wire, respectively, and h and k are the bi-normal and the parallel cooling coefficients. The King's law for the effective velocity dependence of the hot-wire signal E is

$$E^2 = A + BU_{eff}^n , \quad (2)$$

where A, B and n are constants for each hot-wire. Knowing a relative orientation of triple hot-wires, one can find constants for each wire during the calibration procedure and, for given three voltage outputs, reconstruct effective speed at each hot-wire and therefore restore all three components of the velocity. The following values for constants were used, $h = 1.0$, $k = 0.0$ and $n = 0.4$. Summarizing, the calibration procedure is as follows,

1. Find effective cooling speeds, $[U_{eff}^{(1)}, U_{eff}^{(2)}, U_{eff}^{(3)}]^T = C[U, V, W]^T$, where C is a hot-wire angular orientation dependent transformation matrix.
2. Using the least-square estimation, the $A_{(k)}$ and $B_{(k)}$ constants are found,

   $E_{(k)}^2 = A_{(k)} + BU_{eff}^{(k)n}$, $k = 1,2,3$.
3. For a given triplet $\{E_{(k)}\}$, effective cooling speeds are calculated, and velocity components are finally restored.

An example of the calibration procedure is given in Figure 3. The King's law dependence can be observed along with the "scatter" expected from the small scale turbulent motions that are not measured by the sonic anemometer.

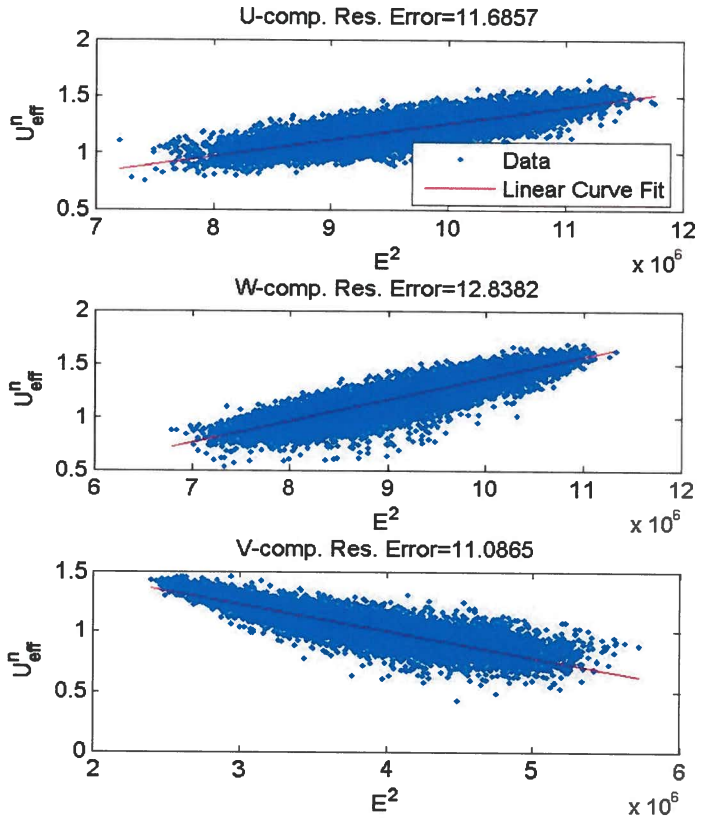

Figure 3 Variation of U^n_{eff} as a function of E^2 for triple hot-wire probe.

Figure 4 shows a comparison between the sonic and hot-wire velocity components. Inspection of this and other time records throughout the measurement period had revealed that while reconstructed U- and W-components agree fairly well with sonic data, the V-component (vertical) hot-wire data follows the sonic velocity trends, but underestimates the amplitude of sonic V-component. An inspection of auto spectra of both sonic and hot-wire velocity data shows that sonic data are spectral aliased, which is indicated by an energy build-up near the end of the sonic resolved spectrum below 30 Hz, see Figure 5. Also, the analysis of velocity-temperature correlations, which is presented later in Figure 6 and 7, has shown that the sonic data are corrupted above 5 to10 Hz. Most probably the reason for this is the sonic anemometer low sampling frequency (60Hz), which leads to the spectral leakage and data corruption for frequencies above 10 Hz.

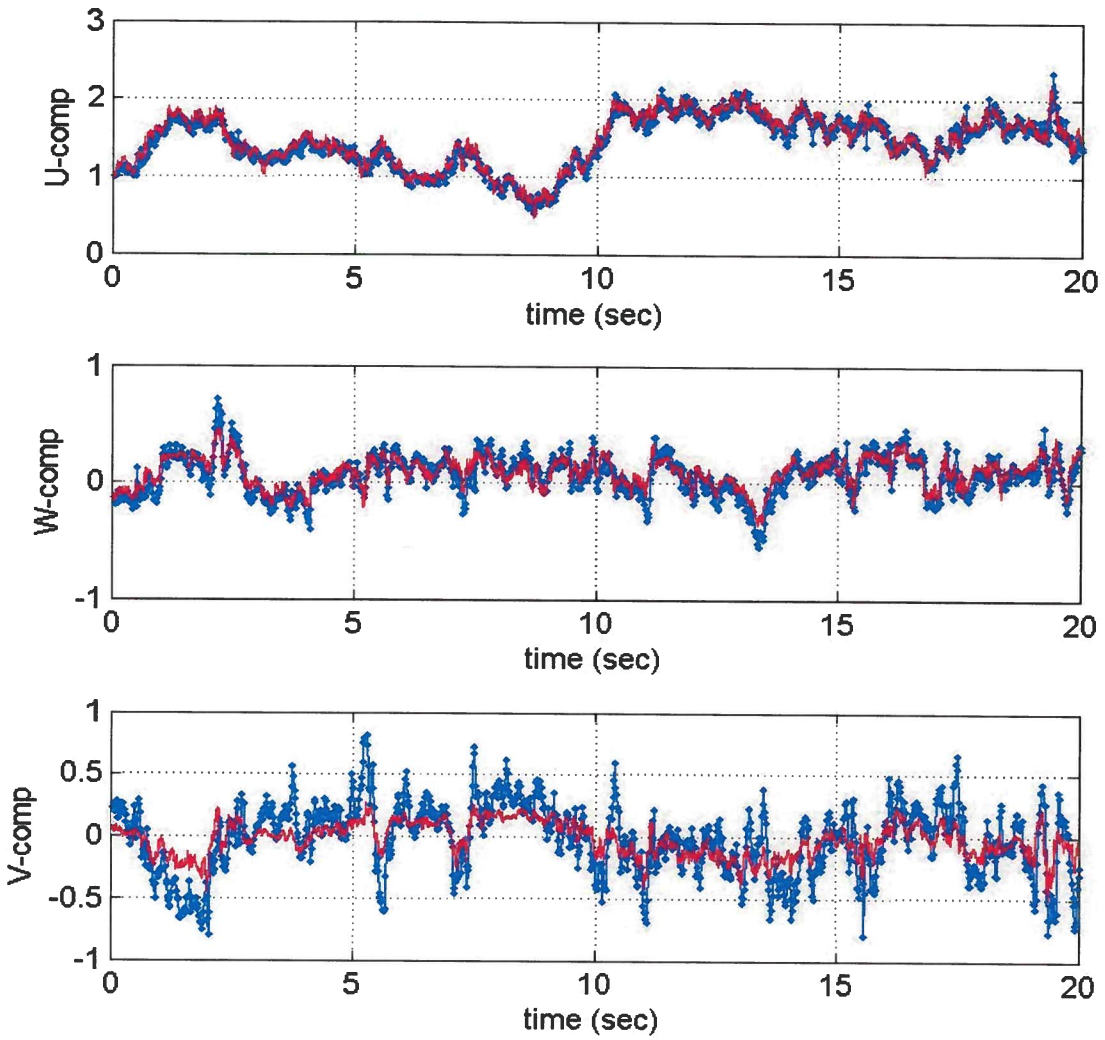

Figure 4 Comparison between sonic velocity (blue line with markers) and hot-wire velocity components (red solid line).

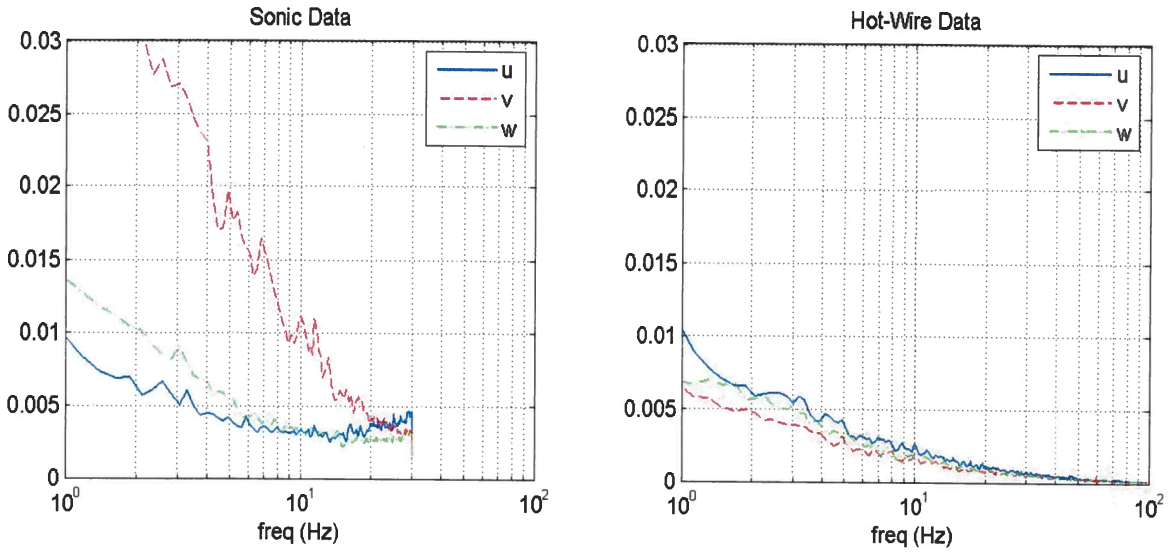

Figure 5 PSD of sonic (left plot) and hot-wire (right plot) velocity components.

Velocity and temperature U-V and V-T spectral correlations were computed from both hot-wire and sonic anemometry and results are shown in Figure 6 and 7 for two different time samples during the measurement period. The first data record (starting 20:48 GMT), presented in Figure 6 was taken before the sunset, so V-T correlations should be in phase. The second set of measurements (starting 01:18 GMT), see Figure 7, were taken at night after the sunset so V-T correlations are out of phase. Indeed, that is exactly the case for the hot-wire data. Most of the correlations lie below 5 to10 Hz in the frequency domain. U-V correlations should be always opposite in phase, which can be observed in both Figures 6 and 7. Analysis of sonic anemometer data of the same time intervals reveals that they exhibit a spurious hump in the correlation amplitude for the range of frequencies between 5 and 30 Hz, and the phase drifts away for the hot-wire-based phase above 5 Hz. Especially it can be observed for U-V spectral correlations, when sonic-based U- and V-components are π out-of-phase for low frequencies (below 5 Hz), in agreement with the hot-wire results, but become $\pi/2$ out-of-phase above 5 Hz. Sonic-based V-T correlations also drift away from either in-phase before the sunset (Figure 6) or out-of-phase after the sunset (Figure 7) values to a $-\pi/2$ value above 5 Hz. It strongly suggests that the sonic data are corrupted or spectral aliased above 5 Hz and all sonic-based results at this test should be approached with a great deal of caution.

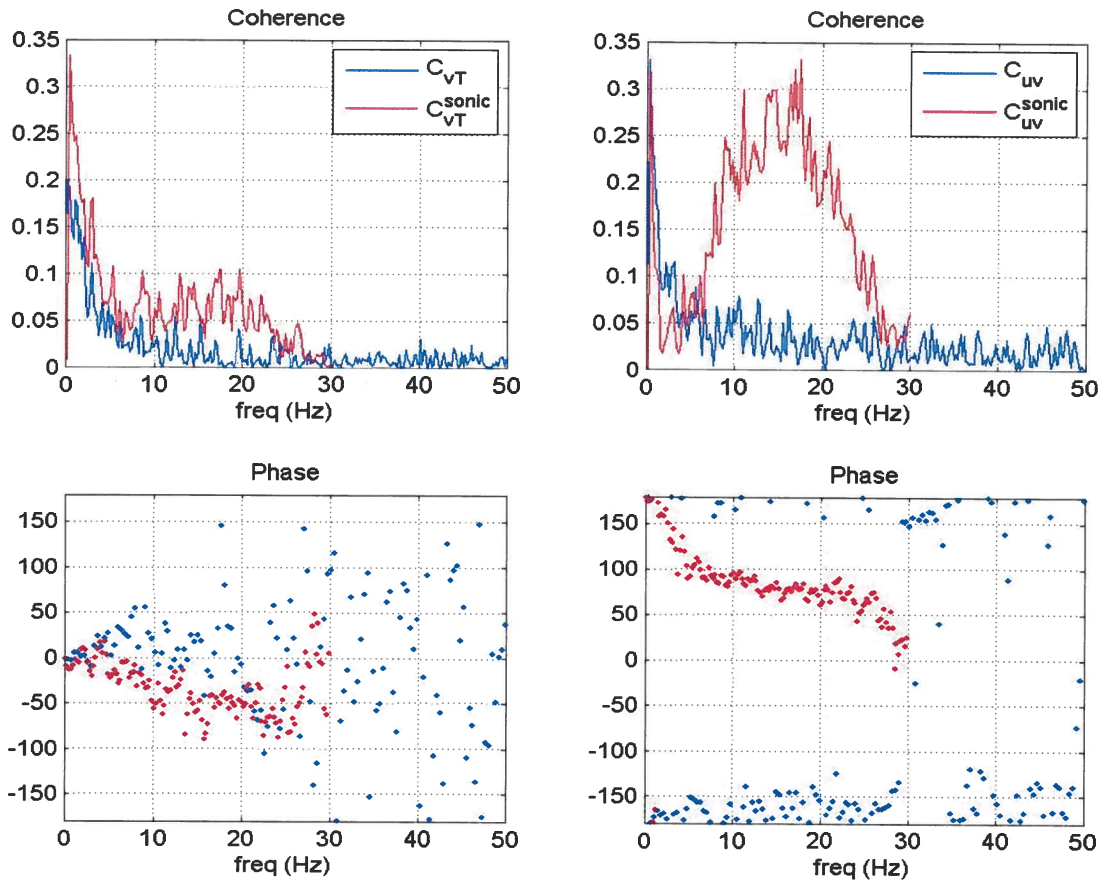

Figure 6 V-T and U-V spectral correlations for hot-wire and sonic data at 20:48 GMT.

Integral time scales can be estimated from velocity series by calculating a time-delayed auto-correlation function. Results for all velocity components and temperature are shown in Figure 8 for two different time records, one before the sunset (left plot) and one after the sunset (right plot) for both hot-wire and sonic anemometer data. Sonic and hot-wire results indicate reasonable agreement. All auto-correlation curves have sharp drops in correlation values for short (less than a second) time delays, followed by a more moderate decrease and eventually approach zero correlation values for time delays of 5-10 seconds. It suggests the presence of many time scales in the flow, ranging from very small (< 1sec) to several seconds. Using Taylor's frozen convective hypothesis and taking a convective speed to be approximately 2 m/sec, one can estimate spatial scale range being between less than a meter up to several meters. V-component shows the smallest ~ 1 sec

time scales, compared with a larger time scale range for U- and W-components, as well as temperature time scales. Also analysis of all time records has shown that time scales and therefore spatial scales are generally smaller after the sunset that before the sunset. Finally, correlation delays faster after the sunset, suggesting smaller range of time/space scales.

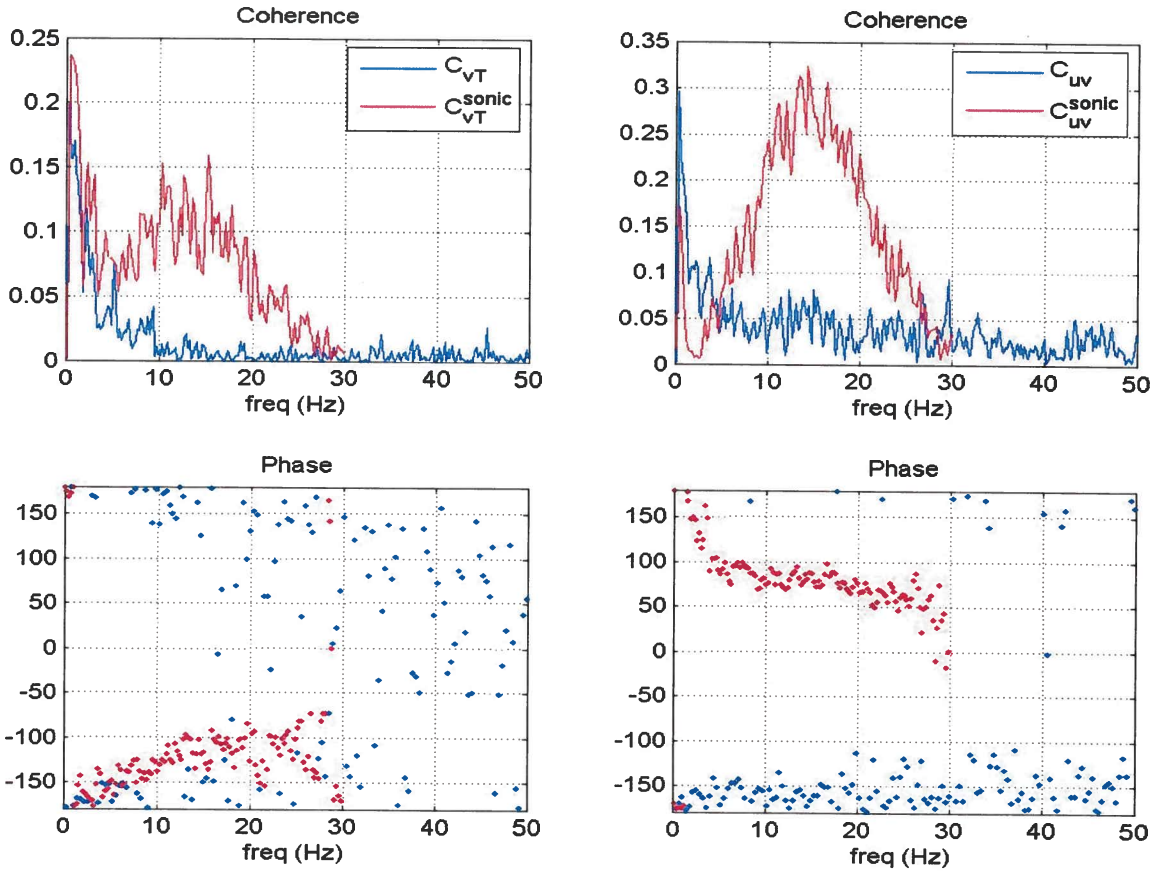

Figure 7 V-T and U-V spectral correlations for hot-wire and sonic data at 01:18 GMT.

All these observations are quite consistent with two different atmospheric conditions. Before the sunset the ground is a heat source, which fuels buoyancy convection near the surface and leads to a formation of relatively large (order of meters) structures. These structures generate, through hydrodynamic instabilities, smaller structures with a wide range of scales. After the sunset the heat source is turned off and the atmospheric conditions quickly become stable. The larger buoyant driven structures no longer form, thus the range of scales of existing structures after the sunset become smaller.

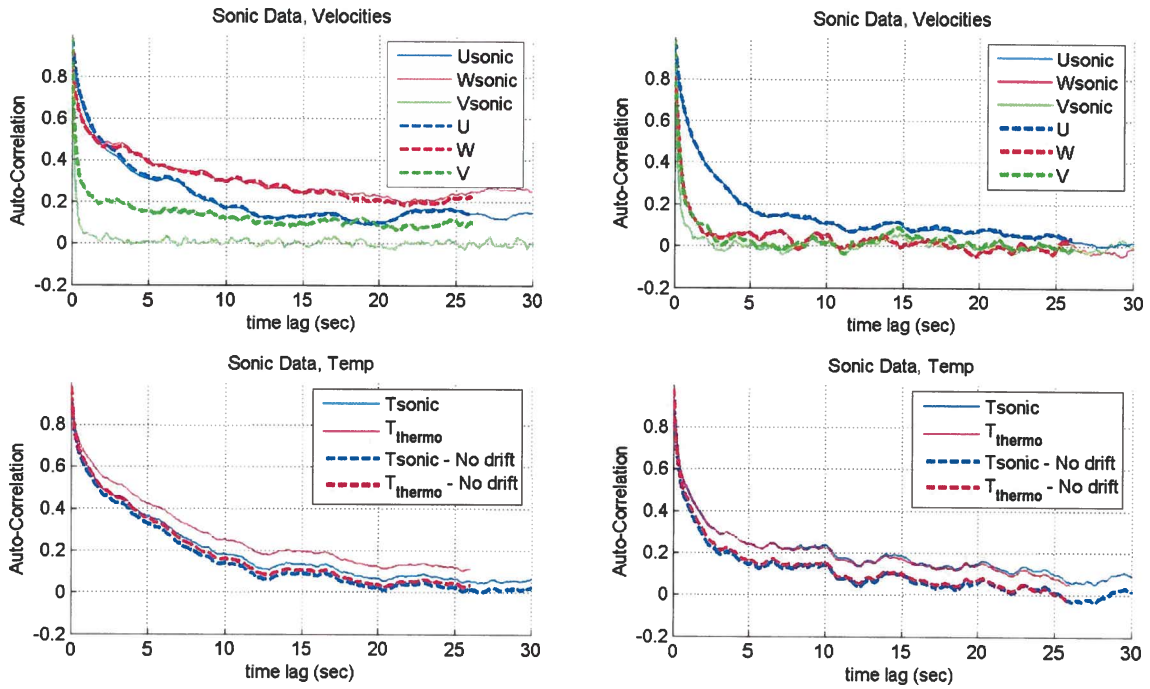

Figure 8 Time-delayed auto-correlation for velocity components and temperature before (left plot) and after (right plot) the sunset.

2.2 Optical-hydrodynamic correlations.

To investigate correlations between local hydrodynamic (velocity, temperature) data and global laser beam degradation while passing through the atmosphere, several parallel IR-laser beams were propagated along the line, where hydrodynamic data were taken, see Figure 9. Variations on laser beams were measured using opto-acoustic sensor SOCRATES [3]. The sensor measures the changes in transit time for laser light traversing between a transmitter and a retro-reflector. Temperature fluctuations, present in the atmosphere lead to density variations along the beam path, thus locally changing the speed of light and the resulting transit time. These changes were recorded at the sampling rate of 11 kHz to a separate computer and later were synchronized with hydrodynamic data using UTC protocol. Several beams were propagated near hydrodynamic measurement stations and the variations on the closest beam were re-sampled to match the hydro-

dynamic sampling rate of 769 Hz and various correlations between laser beam and velocity-temperature were calculated. The source term for temperature changes is the temperature flux

$$q' = \rho c_p V'T' \tag{3}$$

so it was correlated with changes in the laser propagation time.

Unfortunately, no data were taken before the sunset, so all results presented below are for after the sunset period only.

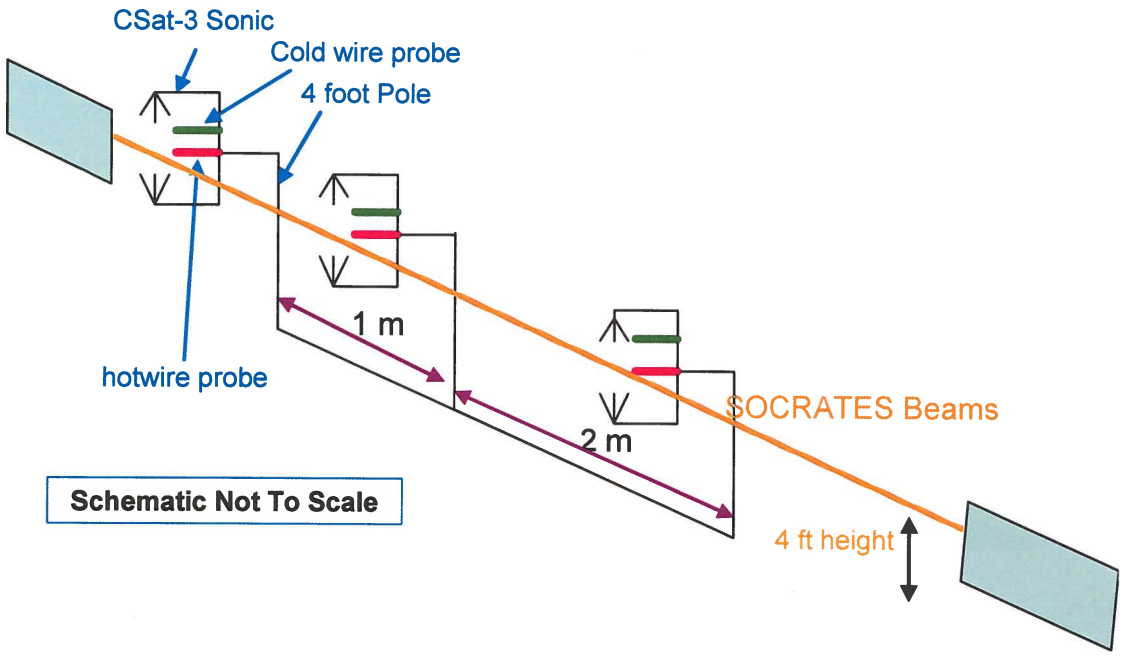

Figure 9 Simultaneous Optical-hydrodynamic experimental set-up.

Power spectra of vertical velocity V, temperature T and the optical signal are presented in Figure 10, upper plot. The optical signal spectrum has a strong peak around 9 Hz, most probably from vibrations of mounting towers, while neither velocity nor temperature spectra exhibit any single peaks. Normalized spectral correlation between V'T' and optical signal is presented in Figure 10, middle plot. For comparison, the spectral correlation between V and T is presented in the same Figure. Velocity-temperature spectral correlation has non-zero correlations at low frequencies below 5 Hz, as it has been discussed in the previous section but there are no significant correlations, less that few percent, between the heat flux and the optical signal. Extensive inspection of all data for all beam revealed no consistent correlations in the frequency domain. Lower plot in

Figure 10 shows a time-delayed normalized correlation between the heat flux and the optical signal (labeled HW-Phase), as well as a temporal derivative of the optical signal (labeled HW-Defl), and it also revealed lack of significant correlations.

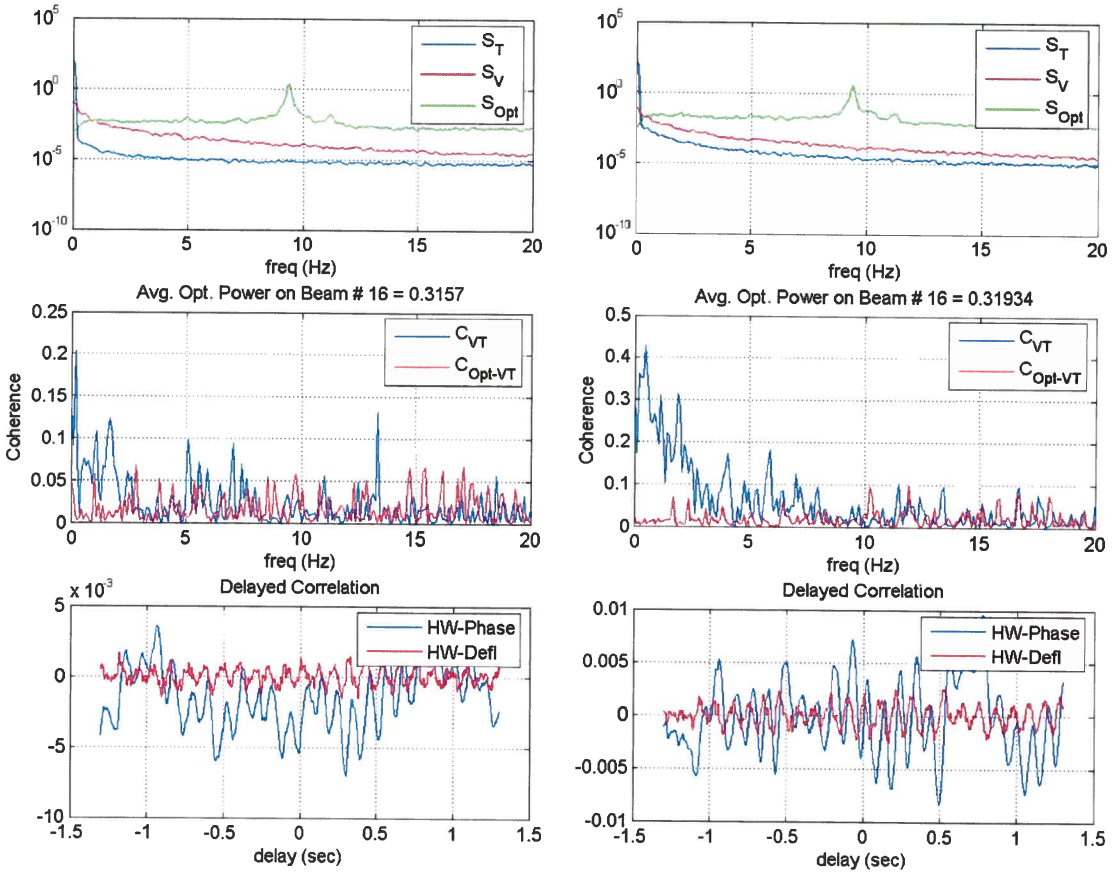

Figure 10 Two examples of hydrodynamic-optical correlation results. Upper plot - power spectra for velocity, temperature and optical signal, middle plot – normalized spectral correlation between the heat flux and the optical signal and lower plot – time-delayed normalized correlation between the heat flux and optical signal (labeled HW-Phase) and the heat flux and the temporal derivative of the optical signal (labeled HW-Defl).

There is no doubt that temperature and heat flux fluctuations affect the laser beam, so the lack of correlation between the optical signal and the temperature flux shows that there is no large-scale structure, but rather many small spatially-uncorrelated randomly distributed structures convecting

over the laser beam at this experiment. Locally correlations may be rather high, but integrating the optical phase over long distances through many uncorrelated optically disturbing events will result in the negligible overall correlation level. The lack of the large-scale structure can also be explained as follows: after the sunset the unsteady buoyancy mechanism is shut down and the atmosphere becomes stable, so the residual turbulent structures simply convect with the flow, gradually break into even smaller structures and eventually dissipate. The conclusions drawn here are therefore only valid during stable atmospheric conditions. It is intuitive that a strongly unstable atmosphere would both provide large RIV induced noise, and would also provide stronger correlation between the local flow field measurements and the optical signals.

3.0 CONCLUSIONS AND RECOMMENDATIONS.

Sampling speed for the sonic anemometer was not high enough to resolve all significant velocity-temperature fluctuations and sonic data were found to be corrupted above 5 Hz. Nevertheless, instantaneous sonic velocity-temperature data were good enough to successfully perform triple hot-wire calibration in-situ and thus allowing to obtain highly resolved time series of velocity-temperature quantities. These hot-wire data were used to calculate various spectral correlations and estimate range of time/space scales in the atmosphere at measurement station locations.

Atmospheric conditions were found to be different before and after the sunset. During the day time the surface is s a heat source creating buoyancy instabilities in the boundary layer near the ground. It creates a wide range of structures, the biggest to be estimated as a few meters in size. After the sunset the convection-related instabilities quickly die down and the structures exhibit a smaller range of different scales.

Unfortunately, all optical data were taken after the sunset, where large-scale structures start breaking apart and become even more uncorrelated spatially. Therefore, both spectral and time-delayed correlations in the physical domain reveal no significant correlations between local quantities, like the heat flux and the global optical signal.

The following recommendations can be made for future tests:

1. A significant increase in the number of hydrodynamic measurement stations should be considered in order to obtain simultaneous velocity-temperature data along the laser beam path. This will allow for greater understanding of the horizontal correlation magnitudes, and will allow for an estimate of the RIV noise to be constructed by integrating along the laser path.
2. The fluid motions in the near surface atmospheric boundary layer are very sensitive to the thermal stability. Measurement throughout a range of conditions from unstable to stable would allow for a greater understanding of these effects on the optical aberrations.
3. The laser measurements and hydrodynamic measurements should be as aligned as possible. Given the present conclusions regarding the length scales of the flow field, it is likely that slight misalignments will lead to decorrelation between the hydrodynamic information and the optical measurements.
4. In addition to the physical alignment of the measurements, it is essential to synchronize the optical and hydrodynamic data to within a fraction of a second. This will allow for a more accurate snapshot of the flow mechanisms involved with the optical aberrations.

4.0 REFERENCES.

1.A. an Dijk, F.T.M. Nieuwstadt, "The Calibration of (Multi-) Hot Wire Probes. 1 Temperature Calibration", Experiments in Fluids, 36, 2004, pp. 540—549.

2.A. an Dijk, F.T.M. Nieuwstadt, "The Calibration of (Multi-) Hot Wire Probes. 1 Velocity Calibration", Experiments in Fluids, 36, 2004, pp. 550—564.

3.Neal. E. Fine and David C. Kring, "Opto-Acoustic Tracking of Aircraft Wake Vortices", AIAA Paper 2005-2965, Monterey, CA, May 2005.